ELSEVIER

Hole-level structure of double δ-doped quantum wells in Si: The influence of the split-off band

I. Rodríguez-Vargas, L.M. Gaggero-Sager*

Facultad de Ciencias, Universidad Autónoma del Estado de Morelos, Av. Universidad 1001, Col. Chamilpa, 62210 Cuernavaca, Mor., Mexico

Abstract

We present the electronic structure calculation of two closely p-type δ-doped quantum wells within the lines of the Thomas–Fermi–Dirac (TFD) theory. The distance between the impurity planes as well as the impurity density of the δ-doped wells is varied. The exchange effects are also considered in the present study. We have paid special attention to the split-off band and its influence on the subband hole levels. We also calculate the mobility ratio of double δ-doped (DDD) quantum wells in Si with respect to a single δ-doped (SDD) one, finding the optimum distance between the wells for maximum mobility. Our results are in a good agreement with respect to the experimental data available.
© 2006 Elsevier B.V. All rights reserved.

1. Introduction

Ultrathin semiconducting layers with exceptional quality can be obtained with the use of modern crystal growth techniques, and impurity seeding is achieved up to the atomic layer scale (δ-doping). Studies of p-type B δ-doped Si quantum wells have been reported [1–5]. Due to the technological importance of this material and the particular properties of the δ-doped systems, they appear to be of interest to the electronic device industry and for basic investigation as well.

The knowledge of energy-level structure is important from theoretical aspects as well as for potential device applications. In particular, the B δ-doped Si QW has been recently investigated from the theoretical and experimental points of view [1–10]. It is clear that in the case of p-type systems the simultaneous consideration of the heavy and light hole bands is unavoidable because the electric charge is distributed among them. Some works [5,6] have shown that, even at $T = 0 \, \mathrm{K}$, the contribution of the split-off (so)

band turns out to be important when the value of the impurity density p_{2D} is greater or equal to $2 \times 10^{13} \, \mathrm{cm}^{-2}$. The reason for this effect is the relative population of the different bands: for values of p_{2D} above $5 \times 10^{13} \, \mathrm{cm}^{-2}$, the relative occupation number of the so_0 level is greater than the corresponding lh_0 level, and ranks second after the hh_0 population. We have considered the system as isotropic and the bands as independent. The nonparabolicity effect slightly modifies the self-consistent solution, in a similar system [11]. So it is not considered.

On the other hand, an important parameter in all semiconductor systems is the mobility and an improvement in this quality is always desirable. In δ-doped systems, it is possible to achieve this improvement via the coupling of other δ-doped layer [12]. Some works report an improvement of 2–3 times with respect to the SDD [12,13]. Although another group [14] has not found such an increase in the mobility, they have found an increase in the conductivity of 20–30% at 77–300 K, for which the DDD system is more appropriate for technological applications. From the theoretical point of view there are few works on these kinds of systems (in GaAs and ZnSe semiconductors) [15–18].

*Corresponding author. Tel.: +52 777 3297020; fax: +52 777 3297040.
E-mail address: lgaggero@buzon.uaem.mx (L.M. Gaggero-Sager).

In the present work we study the electronic and transport properties of the two-dimensional hole gas in double Si δ-doped quantum wells of the type mentioned above. We have studied in detail the influence of the split-off band onto the electronic structure. As we will show, a quantitative description of the hole levels, leading to an excellent agreement with experimental results for optical and transport measurements, can be obtained via the local density Thomas–Fermi–Dirac (TFD) approximation for the inhomogeneous hole gas with three independent and parabolic bands (hh + lh + so) in the quantum wells. For the mobility calculations, we have used a formula previously proposed and applied in GaAs and ZnSe systems [16,18]. This formula has given reliable results with respect to the experimental data available [14,16].

The present paper is arranged as follows: in the next section we present the TFD formalism and the formula for the mobility, followed by results, and concluding with some remarks.

2. Method and model

The TFD energy functional (E_{TFD}) must be constructed. Here and henceforth we assume it to be in the low-temperature limit. Therefore the kinetic energy can be written as [19]

$$t = \frac{3[3\pi^2\hbar^3 p(r)]^{2/3}}{10m_{\text{hh}}m_a},\tag{1}$$

with $m_a = [1 + (m_{\text{lh}}/m_{\text{hh}})^{3/2} + (m_{\text{so}}/m_{\text{hh}})^{3/2}]^{2/3}$, where m_{hh}, m_{lh} and m_{so} are the heavy, light and split-off hole masses, respectively. The kinetic energy functional is

$$T = \int p(\mathbf{r})t\,d\mathbf{r} = \frac{3}{10m_{\text{hh}}m_a}\int p(z)[3\pi^2\hbar^3 p(z)]^{2/3}\,dz.\tag{2}$$

The energy functional of the hole–hole interaction is [18]

$$V_{\text{hh}} = -\frac{e^2\pi}{\varepsilon_{\text{r}}}\iint p(z)p(z')|z - z'|\,dz\,dz'.\tag{3}$$

The interaction between the hole gas and the two impurity planes is described by

$$\begin{aligned}V_{\text{hn}} &= \int p(r)V_N(r)\,dr\\ &= \frac{2e^2\pi}{\varepsilon_{\text{r}}}\left(p_{2D}^1\int p(z)|z + l/2|\,dz\right.\\ &\left.+ p_{2D}^2\int p(z)|z - l/2|\,dz\right),\end{aligned}\tag{4}$$

where $p(r)$, ε_{r}, l, p_{2D}^1 and p_{2D}^2 are the hole density, the relative dielectric constant (hidrogenic model), the inter-layer distance between the wells, the impurity spikes in wells 1 and 2, respectively. The exchange energy for a hole gas with valence band coupling is [20,21]

$$\varepsilon_x(\mathbf{r}) = -\varsigma(w)\frac{3a_0^*}{2\pi}(3\pi^2 p(\mathbf{r}))^{1/3}R_y^*,\tag{5}$$

where

$$\begin{aligned}\varsigma(w) = 2^{-1/3} &+ (1 - w^2)[w^2(aw + b)\\ &+ c(4w^3 + 3w^2 + 2w + 1)],\end{aligned}\tag{6}$$

with $w = m_{\text{lh}}/m_{\text{hh}}$, $a = 0.679$, $b = -0.0686$ and $c = -0.0811$. The exchange functional is

$$E_x = \int p(\mathbf{r})\varepsilon_x(p(\mathbf{r}))\,d\mathbf{r},\tag{7}$$

substituting Eq. (5) in Eq. (7)

$$E_x = -\varsigma(w)\frac{3a_0^*}{2\pi}R_y^*\int p(z)(3\pi^2 p(z))^{1/3}\,dz.\tag{8}$$

Adding the above mentioned terms, E_{TFD} is

$$\begin{aligned}E_{\text{TFD}} &= \frac{3}{10m_{\text{hh}}m_a}\int p(z)[3\pi^2\hbar^3 p(z)]^{2/3}\,dz\\ &- \frac{e^2\pi}{\varepsilon_{\text{r}}}\iint p(z)p(z')|z - z'|\,dz\,dz'\\ &+ \frac{2e^2\pi}{\varepsilon_{\text{r}}}\left(p_{2D}^1\int p(z)|z + l/2|\,dz\right.\\ &\left.+ p_{2D}^2\int p(z)|z - l/2|\,dz\right)\\ &- \frac{3a_0^*\varsigma(w)R_y^*}{2\pi}\int p(z)(3\pi^2 p(z))^{1/3}\,dz.\end{aligned}\tag{9}$$

It is well known that if we apply the variational principle $\delta(E_{\text{TFD}} - \mu N) = 0$ and calculate it by standard procedure we find the Lagrange multiplier μ, identifying it as the chemical potential. If we consider the effective units $R_y^* = e^2/(2\varepsilon_{\text{r}}a_0^*)$ and $a_0^* = \varepsilon_{\text{r}}\hbar^2/(e^2 m_{\text{hh}})$, defining $p_{au}(z) = (a_0^*)^3 p(z)$ it is possible to write the chemical potential as [18]

$$\begin{aligned}\mu = \left[\frac{3\pi^2 p_{au}(z)}{m_a^{3/2}}\right]^{2/3}&R_y^* + V_H(z)\\ &- \frac{2\varsigma(w)}{\pi}(3\pi^2 p_{au}(z))^{1/3}R_y^*.\end{aligned}\tag{10}$$

Solving the quadratic equation for $p_{ua}(z)$ in Eq. (10) and the remaining with the physically meaningful solution

$$p_{au}(z) = \frac{m_a^3\varsigma^3(w)}{3\pi^5}\left[1 - \sqrt{1 + \frac{\pi^2(\mu^* - V_H^*(z))}{\varsigma^2(w)m_a}}\right]^3,\tag{11}$$

where $V_H^* = V_H/R_y^*$ and $\mu^* = \mu/R_y^*$. Replacing $p_{ua}(z)$ in the Poisson equation, and if the impurity concentration is the same in both wells ($p_{2D}^1 = p_{2D}^2 = p_{2D}$), the system is symmetric with respect to the central point, so, the Hartree potential is an even function and we can work with only one side ($z \leqslant 0$).

$$\begin{aligned}\frac{d^2 V_H^*(z)}{dz^2} &= -\frac{8m_a^{3/2}}{3\pi}(\mu^* - V_H^*(z))^{3/2}\\ &+ 8\pi p_{2D}\delta(z + l/2),\end{aligned}\tag{12}$$

the specific and physically meaningful solution of this type of equation is of the form $1/f^4(z)$, where $f(z)$ is a linear function of z. In the case of double δ-doped QWs the

solution is [18]

$$V_H^*(z) - \mu^* = -\frac{\alpha^2}{(\alpha|z + l/2| + z_0)^4}, \tag{13}$$

substituting Eq. (13) into Eq. (12), we find α,

$$\alpha = \frac{2m_a^{3/2}}{15\pi}, \tag{14}$$

and the neutrality charge requirement gives

$$z_0 = \left(\frac{\alpha^3}{\pi p_{2D}}\right)^{1/5}. \tag{15}$$

Substituting Eq. (13) in Eq. (11), the charge density is

$$p_{au}(z) = \frac{m_a^3 \varsigma^3(w)}{3\pi^5} \left[1 - \sqrt{1 + \frac{\pi^2}{\varsigma^2(w)m_a} \frac{\alpha^2}{(\alpha|z + l/2| + z_0)^4}}\right]^3. \tag{16}$$

The exchange potential takes the form [18]

$$V_x^*(z) = -\frac{2\varsigma^2(w)m_a}{\pi^2}\left[1 - \sqrt{1 + \frac{\pi^2}{\varsigma^2(w)m_a} \frac{\alpha^2}{(\alpha|z + l/2| + z_0)^4}}\right]. \tag{17}$$

At low temperatures, the Fermi level is located at only a very few meV above the band's edge [18]. Therefore it is a good approximation to take it as coinciding with the potential well vertex. Finally, the total potential, $V^*(z) = V_H^*(z) + V_x^*(z)$, is

$$V^*(z) = -\frac{\alpha^2}{(\alpha|z + l/2| + z_0)^4} - \frac{2\varsigma^2(w)m_a}{\pi^2}$$
$$\times \left[1 - \sqrt{1 + \frac{\pi^2}{\varsigma^2(w)m_a} \frac{\alpha^2}{(\alpha|z + l/2| + z_0)^4}}\right]. \tag{18}$$

The last equation summarizes the model for the total potential of p-type DDD Si QWs. Such an equation is substituted into three uncoupled Schrödinger like equations in order to obtain the heavy, light and split-off hole ladders. This way we can avoid a troublesome and long self-consistent calculation.

The TFD method also allows us to study the transport properties of the system. We only consider the ionized acceptor scattering mechanism because it is the most important one at low temperatures. The Coulomb scattering potential due to ionized impurities is considered as distributed randomly in the doped layer. We have taken the ratio of the mobility of DDD to SDD QWs [16].

In Ref. [1] the influence of the temperature onto the electronic structure has been calculated. The results have shown a slightly modification of the level structure when the temperature is less than 6 meV (77 K). In such a case the electronic structure can be taken as that corresponding to 0 K and the thermal effect can be considered as a charge redistribution. Then, the mobility expression can be written

as [16,18]

$$\mu_{rel}^\delta = \frac{\sum_j m_j^* \sum_i \int |F_e^\delta(z')|^2 In[1 + e^{(k_F^\delta - E_i^\delta)/k_B T}]|z'|\,dz'}{\sum_j m_j^* \sum_i \int |F_e^{2\delta}(z')|^2 In[1 + e^{(k_F^{2\delta} - E_i^{2\delta})/k_B T}](|z' - l/2| + |z' + l/2|)\,dz'}, \tag{19}$$

where $F_e^\delta(z')$, k_F^δ and E_i^δ ($F_e^{2\delta}(z')$, $k_F^{2\delta}$ and $E_i^{2\delta}$) are the envelope function, the Fermi level and the ith level, respectively, of the SDD (of DDD).

3. Results and discussion

The different ladders of levels are calculated by putting in the wave equation the corresponding values of m^*: m_{hh}^*, m_{lh}^* and m_{so}^*. The following input parameters were used: $m_{hh}^* = 0.52m_0$, $m_{lh}^* = 0.16m_0$, $m_{so}^* = 0.23m_0$, m_0 being the free electron mass and $\varepsilon_r = 11.7$. It is important to mention that we have chosen an electronic point of view; this means that the hole subband levels and the potential profile will be depicted as in the case of electrons, and in such a case all energies will be negative. We also mention that our system is ideal, so the doping thickness is zero. The aforementioned comments are consistent with the derivation of the potential that represents the band bending as it was detailed in the previous section.

Figs. 1 and 2 depict the hole energy-level structure versus the interlayer distance between wells, omitting and take into account the split-off band in the calculation. We have found the splitting in the hole energy-level structure, due to the interaction between δ wells. The splitting starts at different distances for the different levels. The splitting of the heavy and light hole ground levels takes place at small distances because the overlapping between the wave functions of the δ wells is greater when the wells are closer. For the excited levels the splitting distance is larger, since the penetration into the barrier is greater, the higher the level is. Comparing Figs. 1 and 2, we can see (from the
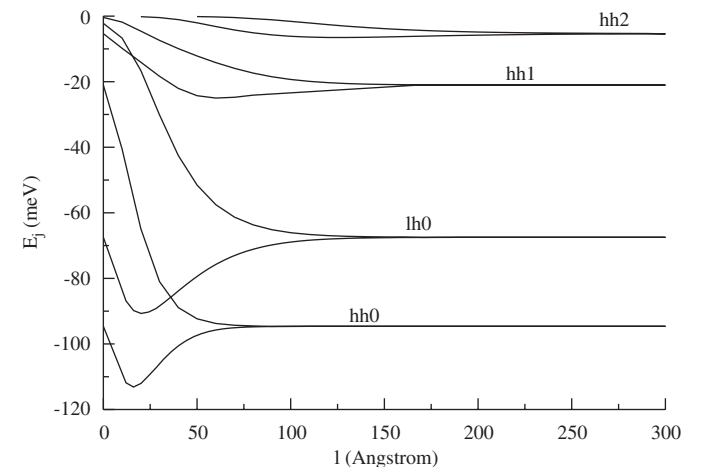

Fig. 1. Hole energy levels versus the distance between the impurity planes l, for an impurity density $p_{2D} = 20 \times 10^{12} \, cm^{-2}$, omitting the split-off band.
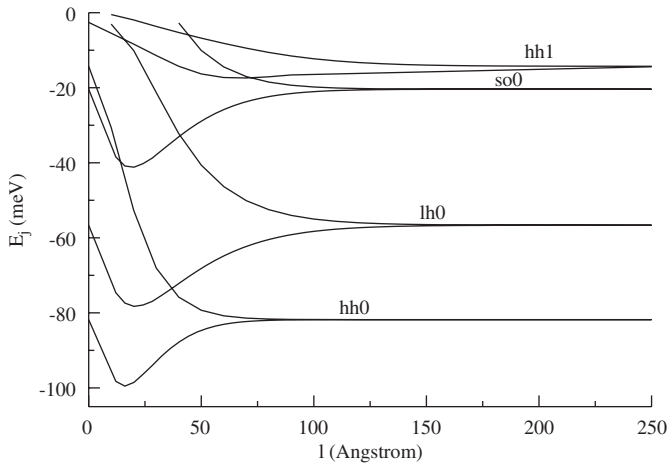
Fig. 2. Hole energy levels versus the distance between the impurity planes l, for an impurity density $p_{2D} = 20 \times 10^{12} \, \text{cm}^{-2}$, taking into account the split-off band.
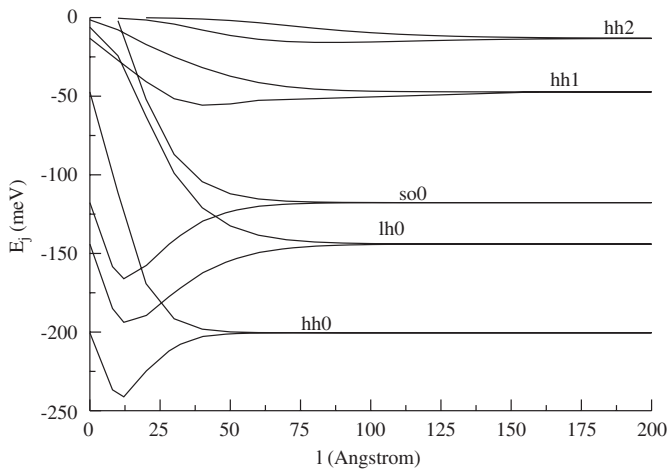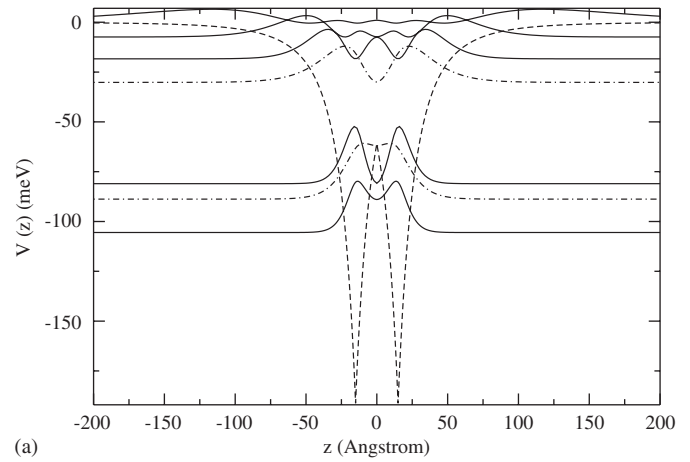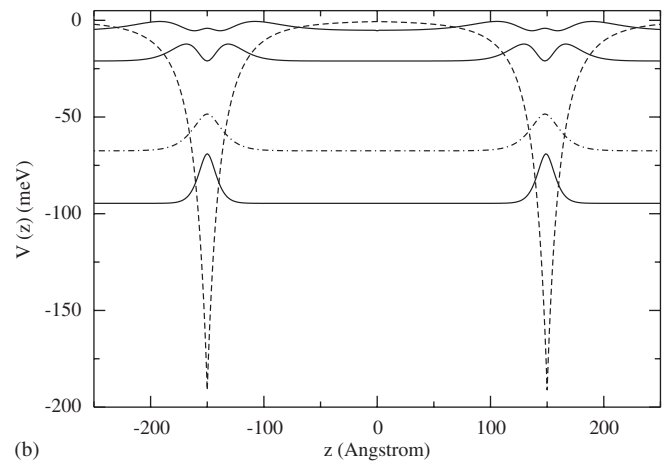

Fig. 3. Hole energy levels versus the distance between the impurity planes l, for an impurity density $p_{2D} = 60 \times 10^{12} \, \text{cm}^{-2}$, taking into account the split-off band.

Fig. 4. Potential profile (dashed line) and the square of the wave functions for the heavy (solid lines) and light holes (dashed-dot lines) for: (a) $l = 30 \, \text{Å}$ and (b) $l = 300 \, \text{Å}$ for $p_{2D} = 20 \times 10^{12} \, \text{cm}^{-2}$, omitting the split-off band.

energetic scale) that omitting the split-off band, the heavy and light hole levels are more confined. However, the degeneration distance (this is when the level splitting is practically null) remains unchanged for these levels. But the presence of the split-off levels is a very important feature. The splitting of these levels takes place, even, at a distance lesser than the basic light hole one.

On the other hand, an increase in the impurity density brings with itself an extra confinement, due to the potential depth increases. Besides, eventually more levels will be trapped and the degeneration distance will be lesser, Fig. 3. In Figs. 4–6 we present the potential profile and the square of hole wave functions for two different distances (close and far) between wells. The impurity densities in Figs. 4, 5 and 6 are the same as that in Figs. 1, 2 and 3, respectively. When the δ-doped wells are close to each other the splitting of levels is evident, due to strong interaction between the

wells, Figs. 4a, 5a and 6a, while for large distances the energy levels are practically degenerate, Figs. 4b, 5b and 6b.

In Tables 1 and 2, we present the potential depth and the transitions of the different levels to the heavy ground one, with and without the split-off band for $l = 0 \, \text{Å}$. We have found a reduction in the potential depth in the three band calculations, therefore a reduction in the energy transitions, see Tables 1 and 2. We have found a difference of 2 meV for ΔE_{hl00} with and without the split-off band for an impurity density of $20 \times 10^{12} \, \text{cm}^{-2}$. Increasing the density up to $90 \times 10^{12} \, \text{cm}^{-2}$ a difference of 5.2 meV is found for the same transition. For transitions with higher levels (ΔE_{hh01}, ΔE_{hh02}, etc.) the difference is more pronounced.

Karunasiri [4] has performed measurements of the intersubband absorption coefficient for a quantum well of B in a Si matrix at room temperature as a function of the photon energy. The sample considered in that study consisted of 10 periods of 3.5 nm thick heavily doped Si layers separated by 30 nm thick undoped Si barriers. The absorption peak corresponding to an impurity concentration of $9 \times 10^{13} \, \text{cm}^{-2}$ is located at $\approx 270 \, \text{meV}$ and has a
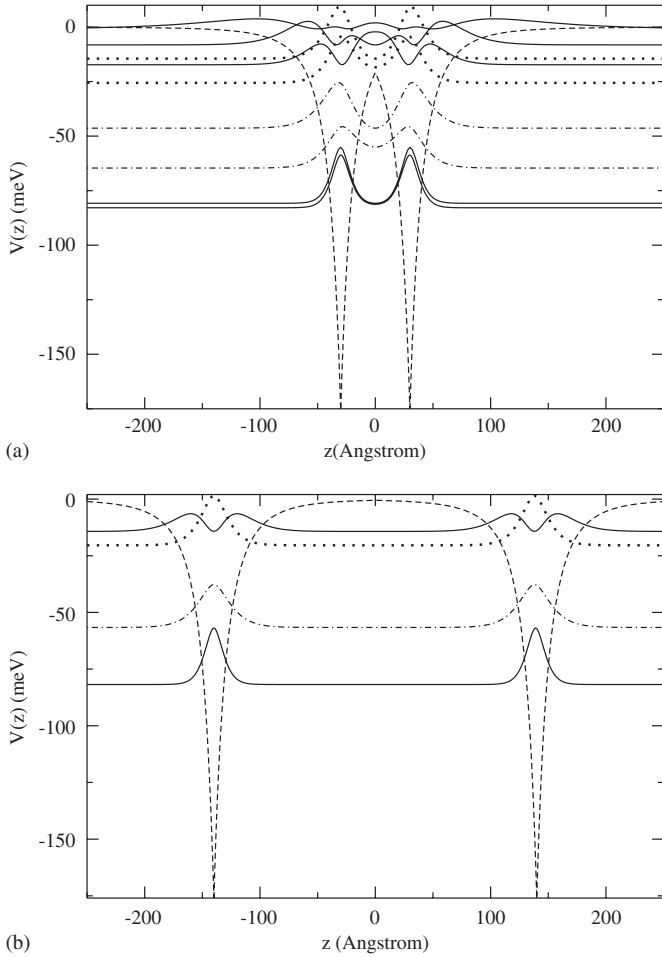
Fig. 5. Potential profile (dashed line) and the square of the wave functions for the heavy (solid lines), light (dashed-dot lines) and split-off holes (dot lines) for: (a) $l = 60\,\text{Å}$ and (b) $l = 280\,\text{Å}$ for $p_{2D} = 20 \times 10^{12}\,\text{cm}^{-2}$, taking into account the split-off band.
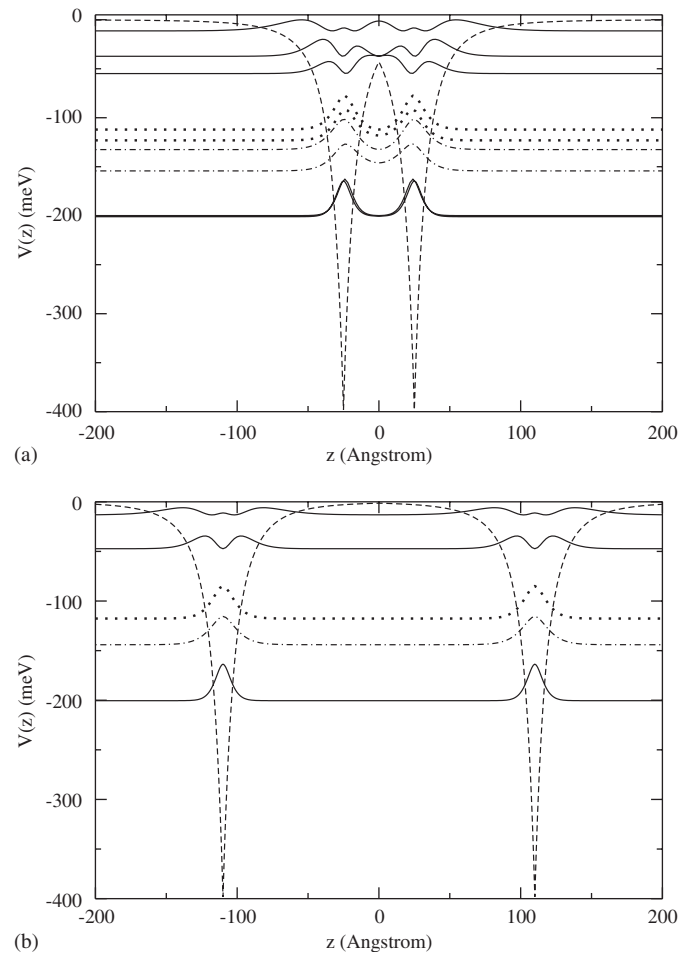

Fig. 6. Potential profile (dashed line) and the square of the wave functions for the heavy (solid lines), light (dashed-dot lines) and split-off holes (dot lines) for: (a) $l = 50\,\text{Å}$ and (b) $l = 220\,\text{Å}$ for $p_{2D} = 60 \times 10^{12}\,\text{cm}^{-2}$, taking into account the split-off band.

width of $\approx 200\,\text{meV}$. According to our calculations ($l = 0$), the transition energy hh$_0$–hh$_3$ equal to $274.3\,\text{meV}$ seems to be the fundamental transition contributing to the assertion peak. It is important to mention that this result for the fundamental transition reflects the importance of the exchange effects, since ignoring the many-body contribution a value of $294.3\,\text{meV}$ ($l = 0$) is obtained for the same transition in a self-consistent calculation [6]. As it was mentioned, the absorption peak reported in Ref. [4] is a broad one, and that feature could be explained by considering that, besides the fundamental transition discussed above, there also exist other transitions like hh$_0$ $-$ lh$_2$ $= 268.2\,\text{meV}$ ($l = 0$), which could contribute to the absorption peak, although their population factors are not large enough and, therefore, their relative importance should be small.

Zhu et al. [2] made B-δ-doped Si with a Schottky barrier. They showed shifts of the conductance peaks in the spectra with a peak doping concentration of $p_{3D} = 2 \times 10^{20}\,\text{cm}^{-3}$, and doped thickness of $1.2\,\text{nm}$. The activation energy is $110 \pm 20\,\text{meV}$. The difference between the basic level and

Table 1
Potential depth and the transitions of the levels to the heavy ground one ($l = 0$): $\Delta E_{hl00} = |E_{hh0} - E_{lh0}|$, $\Delta E_{hh01} = |E_{hh0} - E_{hh1}|$, $\Delta E_{hh02} = |E_{hh0} - E_{hh2}|$, $\Delta E_{hl01} = |E_{hh0} - E_{lh1}|$, etc., for different impurity densities p_{2D} ($10^{12}\,\text{cm}^{-2}$), omitting the split-off band

p_{2D}	ΔE_{hl00}	ΔE_{hh01}	ΔE_{hh02}	ΔE_{hl01}	ΔE_{hh03}	V_0
20	27.2	73.6	89.3	92.4		191.2
30	37.1	99.2	122.0	125.8	132.2	258.1
40	45.0	122.2	152.3	158.7	163.8	319.7
50	53.0	144.5	181.0	188.9	195.7	377.8
60	60.5	165.3	208.4	217.8	226.3	433.2
70	67.7	185.3	234.8	245.6	256.0	486.5
80	74.7	204.5	260.4	272.6	284.8	538.2
90	81.4	223.1	285.2	298.9	312.9	588.3

the top of the valence band in our calculations ($l = 0$) is $94.8\,\text{meV}$ with $p_{2D} = 2.4 \times 10^{13}\,\text{cm}^{-2}$, while omitting the exchange effects a difference of $86\,\text{meV}$ ($l = 0$) is obtained [6]. Wang et al. [3] also obtained experimental intersubband absorption spectra in B-δ-doped Si multiple quantum wells. They measured 10 periods of B-doped layers with a width of about $5\,\text{nm}$. They report a transition energy of

Table 2
Potential depth and the transitions of the levels to the heavy ground one ($l = 0$): $\Delta E_{hl00} = |E_{hh0} - E_{lh0}|$, $\Delta E_{hs00} = |E_{hh0} - E_{so0}|$, $\Delta E_{hh01} = |E_{hh0} - E_{hh1}|$, $\Delta E_{hl01} = |E_{hh0} - E_{lh1}|$, etc., for different impurity densities p_{2D} (10^{12} cm^{-2}), taking into account the split-off band

p_{2D}	ΔE_{hl00}	ΔE_{hs00}	ΔE_{hh01}	ΔE_{hh02}	ΔE_{hl01}	V_0
20	25.2	60.4	67.6	79.2		176.1
30	33.3	67.4	91.3	108.8	112.1	237.5
40	41.8	72.9	112.9	136.2	140.9	294.1
50	49.4	78.0	133.7	162.3	168.1	347.4
60	56.4	82.8	152.3	187.2	194.3	398.2
70	58.4	87.4	171.9	211.4	219.4	447.2
80	69.8	91.9	190.0	234.7	244.2	494.5
90	76.2	96.2	207.5	258.3	268.0	540.5

Fig. 8. Mobility calculations versus the interlayer distance between δ-doped wells with $p_{2D} = 60 \times 10^{12}$ cm^{-2}, taking into account the split-off band.
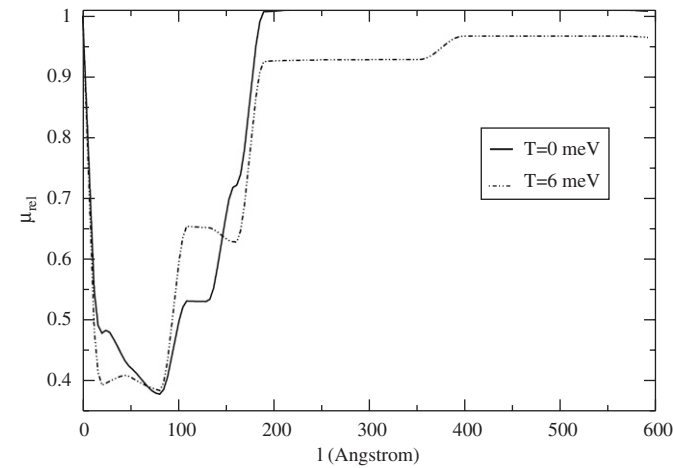

Fig. 7. Mobility calculations versus the interlayer distance between δ-doped wells with $p_{2D} = 20 \times 10^{12}$ cm^{-2}, taking into account the split-off band.

Fig. 9. Mobility calculations versus the interlayer distance between δ-doped wells with $p_{2D} = 80 \times 10^{12}$ cm^{-2}, taking into account the split-off band.

125 meV for a doping density $p_{2D} = 3.5 \times 10^{13}$ cm^{-2}. This is comparable to the transition energy of 128.9 meV obtained in our calculation ($l = 0$) for the transition between the ground level and the top of the valence band. As we can see from the above mentioned results, the inclusion of the exchange effects improves our estimations for the fundamental transitions, compared to the results obtained ignoring such effects [6].

Finally, we present the mobility calculations versus the interlayer distance between wells in Figs. 7, 8 and 9 for 20, 60 and 80×10^{12} cm^{-2}, respectively. We have taken into account the split-off band in the mobility results. As we can see from these figures, the two limiting cases of null and large distance for the mobility are well fulfilled, i.e., the mobility must tend to one, since the hole subband structure for these two cases corresponds to the SDD. Fig. 7 presents a peak at around 120 Å; this peak is directly related to the degeneration distance of the basic level of heavy holes, since when the degeneration takes place a redistribution of the charge density takes place as well. This redistribution of charge favors the higher levels, specially the levels with nodes in the impurity planes. The solid line corresponds to
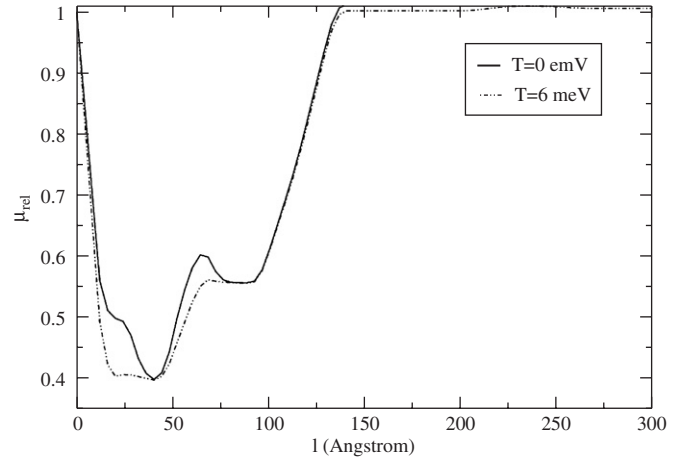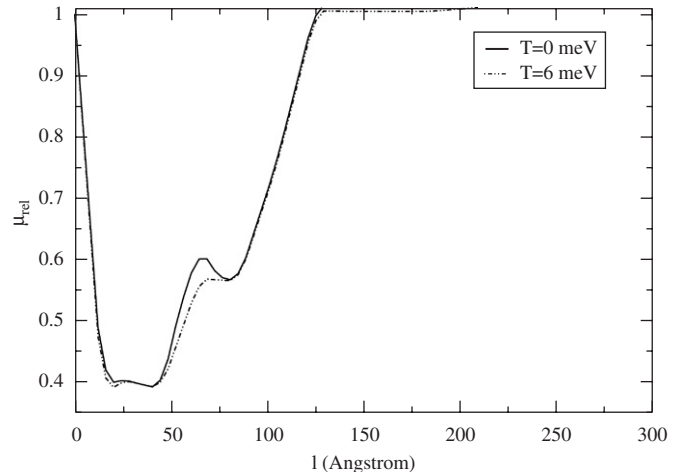
the calculation at 0 K, while the dashed-dot to 77 K (6 meV). The mobility at 0 K presents an important increase in the degeneration distance of the heavy hole basic level (120 Å); however, this lift does not represent a clear peak. Increasing the temperature up to 77 K a peak appears at the same distance, due to the intervention of energy levels above the Fermi level in the mobility calculations. These levels have a probability to be occupied at temperature different from zero, thereby they must be taken into account in the mobility calculations. In this case, we have the first excited heavy hole states above the Fermi level with nodes in the impurity planes. The peak in the mobility is for this reason.

Increasing the impurity density the degeneration distance changes because the potential depth increases as well. Therefore, the peak in the mobility changes to 70 and 60 Å for impurity concentrations of 60 and 80×10^{12} cm^{-2},

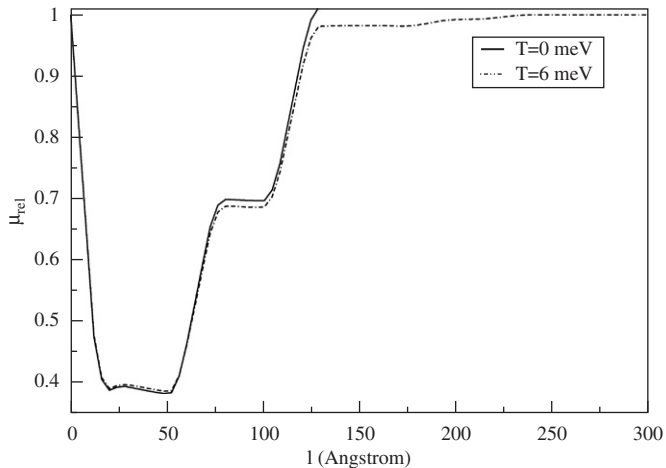Fig. 10. Mobility calculations versus the interlayer distance between δ-doped wells with $p_{2D} = 60 \times 10^{12}\,cm^{-2}$, omitting the split-off band.

Figs. 8 and 9. From 8 and 9, we can see an opposite behavior with respect to Fig. 7, since for $T = 0\,K$ a peak is found for the mobility, while for $T = 77\,K$ this peak is not present. This is explained as follows: the levels that enter in the calculations at $T = 0\,K$ are the basic levels for the three ladders (hh, lh and so) and the first excited heavy hole level; this is the level that favors the mobility, consequently the peak present in Figs. 8 and 9. For $T = 77\,K$, we have levels above the Fermi level with charge localization near the impurity planes, therefore the net effect is the non-appearance of a peak. It is important to stress that the mobility peaks found for these impurity densities are not present in the mobility calculations omitting the split-off band (see Fig. 10 for $p_{2D} = 60 \times 10^{12}\,cm^{-2}$). Comparing the occupation of the energy levels without and with split-off band for $60 \times 10^{12}\,cm^{-2}$ at the degeneration distance, Figs. 8 and 10, a reduction of the occupation of 13.3%, 1.7% and 6.7% is found for the basic level of heavy and light holes, and the first level of heavy holes, when the split-off band is considered. The sum of these reductions coincides with the occupation of the split-off ground level. These reductions and mainly the reduction in the heavy hole ground level favors the mobility, since this level has a major contribution to the dispersion rate.

4. Conclusions

In summary, it is possible to state that TFD calculations for the hole energy levels and relative mobility in p-type double δ-doped quantum wells in Si are plausible and well accurate, and provide a rather simple way of obtaining valuable information of the subband structure and relative mobility in these systems. The split-off band study shows that this band is necessary in the hole-level and mobility calculations.

References

[1] L.M. Gaggero-Sager, R. Pérez-Alvarez, Appl. Phys. Lett. 70 (1997) 212.
[2] J.H. Zhu, D.W. Gong, B. Zhang, F. Lu, C. Sheng, H.H. Sun, X. Wang, Phys. Rev. B 52 (1995) 8959.
[3] K.L. Wang, R.P.G. Karunasiri, J.S. Park, Surf. Sci. 267 (1992) 74.
[4] G. Karunasiri, Jpn. J. Appl. Phys. 33 (1994) 2401.
[5] G.M. Siphai, P. Enderlein, L.M.R. Scolfaro, J.R. Leite, Phys. Rev. B 53 (1996) 9930.
[6] L.M. Gaggero-Sager, M.E. Mora-Ramos, Phys. Stat. Sol. (B) 220 (2000) 163.
[7] J. Caro, I.D. Vink, G.D.J. Smit, S. Rogge, T.M. Klapwijk, Phys. Rev. B 69 (2004) 125324.
[8] P.W. Chien, S.L. Wu, S.C. Lee, S.J. Chang, Mater. Chem. Phys. 77 (2002) 426.
[9] R. Liu, A.T.S. Wee, D.H. Shen, H. Takenaka, Surf. Interface Anal. 36 (2004) 172.
[10] F. Kaesen, C. Fink, K.G. Anil, W. Hansch, T. Doll, T. Grabolla, H. Schreiber, I. Eisele, Thin Solid Films 336 (1998) 309.
[11] G.-Q. Hai, N. Studart, F.M. Peeters, Phys. Rev. B 55 (1995) 8363.
[12] X. Zheng, T.K. Carns, K.L. Wang, B. Wu, Appl. Phys. Lett. 62 (1993) 504.
[13] H.H. Radamson, M.R. Sardela Jr., O. Nur, et al., Appl. Phys. Lett. 64 (1994) 1842.
[14] V.L. Gurtovoi, V.V. Valyaev, S.Yu. Shapoval, A.N. Pustovit, Appl. Phys. Lett. 72 (1998) 1202.
[15] G.-Q. Hai, N. Studart, Phys. Rev. B 52 (1995) 2245.
[16] I. Rodriguez-Vargas, L.M. Gaggero-Sager, V.R. Velasco, Surf. Sci. 537 (2003) 75.
[17] E. Ozturk, Y. Ergun, H. Sari, I. Sokmen, Appl. Phys. A 77 (2003) 427.
[18] I. Rodriguez-Vargas, L.M. Gaggero-Sager, J.C. Martinez-Orozco, Phys. Stat. Sol. (B) 242 (2005) 1043.
[19] S. Lundqvist, N.H. March, Theory of Inhomogeneous Electron Gas, Plenum Press, New York, 1983.
[20] P.A. Bobbert, H. Wieldraaijer, R. van der Weide, M. Kemerink, P.M. Koenraad, J.H. Wolter, Phys. Rev. B 56 (1972) 3664.
[21] M. Combescot, P. Nozi'eres, J. Phys. C 5 (1972) 2369.